RESEARCH PAPER

Engineering Nano-aggregates: β-Cyclodextrin Facilitates the Thiol-Gold Nanoparticle Self-Assembly

D Badmapriya[1], Sameena Yousuf [2,3] Israel VMV Enoch [3,4*]*

[1]Department of Chemistry, School of Advanced Sciences, Vellore Institute of Technology, Vellore, Tamil Nadu, India

[2]Department of Chemistry, Sri Shakthi Institute of Engineering and Technology, Coimbatore 641062, Tamil Nadu, India

[3]Department of Chemistry, 4Nanotoxicology Research Lab, Department of Nanoscience, Karunya Institute of Technology and Sciences, Coimbatore 641114, Tamil Nadu, India

ARTICLE INFO

ABSTRACT

The structure and morphology of nonmaterial formed by colloidal synthesis represent a subject of interest as it is a factor deciding the physicochemical properties and biological applications of nanostructures. Among various nanoparticles, gold can develop fractal assembled patterns. Herein, we report a nano-aggregate of a thiol-on-gold self-assembled structure and the influence of β-cyclodextrin on the self-assembly. The host: guest association of the 5-(4-pyridyl)-1,3,4-oxadiazole-2-thiol is studied using UV-visible, fluorescence spectroscopy and molecular modelling analysis. In free form unbound to gold nanoparticles, the thiol compound forms a cyclodextrin complex with a 1: 1 stoichiometry. The thiol assembled on gold nanoparticles, aggregating to constitute irregular patterns. β-cyclodextrin encapsulates the thiol-on-gold nanoparticles and their morphology changes. The influence of β-cyclodextrin on the aggregation of the thiol guest molecule and the morphology of the thiol-on-gold nanostructure is discussed. The non-covalent complex made up by the thiol molecule with cyclodextrin plays a vital role in tuning the structure of the nanostructure when assembled on gold nanoparticles.The study will open up a significant method in the approach towards site specific drug delivery via a physical encapsulation.

How to cite this article

INTRODUCTION

Microparticulate (0.1–100 µm) and nano-particulate systems (1–100 nm) have gained particular interest in the field of drug delivery [1-4]. Such micro/nanoparticulate drug delivery systems consist of an active ingredient and the host molecules such as cyclodextrins (CDs) which can develop nanosized aggregates in aqueous solutions [5]. CDs can encapsulate guest molecules of appropriate size and shape in its cavity [6-8].

The self-assembly of CDs is influenced by the guest molecule in the host:guest complex [9]. These properties of CDs are used in a substantial number of marketed drugs formulations.

Gold nanoparticles play a principal role in nanoscience and nanotechnology [10-13]. Gold nanoparticles modified with β-CDs on the surface can self-assemble into aggregates via the host–guest complexation between β-CDs and ditopic guests significantly altering the spectroscopic

* Corresponding Author Email: drisraelenoch@gmail.com

properties [14]. For instance, aggregates of metallic nanoparticles provide a higher signal enhancement than well-dispersed nanoparticles combined [15]. Host-guest complexes stabilize the Au nano crystals and provide self-assembly environment for forming nanostructure around Au nanocrystals [16]. Hence efficient drug delivery can be attained on targets by loading maximum amount of drugs onto nano-aggregates. In this paper, we report a novel heterocyclic compound which possesses six-membered and five-membered rings connected and a thiol group (Fig. 1 (a)) which assembles on gold nanoparticle. In addition, we report the influence of the encapsulation of the molecule by β-CD (containing a cavity, Fig. 1 (b)) on forming the nanostructures.

MATERIALS AND METHODS
Materials

5-(4-pyridyl)-1,3,4-oxadiazole-2-thiol (97%, Molecular formula = $C_7H_5N_3OS$, Molecular weight = 179.2),(Compound 1), chloroauric acid (Sigma Aldrich, Bangalore), β-cyclodextrin, and Glucose (HiMedia, Mumbai), were used as received. HPLC grade solvents (Qualigens fine chemicals, India) were used for the study of absorptionand fluorescence spectroscopy.

Methods
Preparation of inclusion complex of β-cyclode-xtrin and 5-(4-pyridyl)-1,3,4-oxadiazole-2-thiol

0.01 M β-CD was dissolved in 40 mL of double distilled water and 0.05 M of 5-(4-pyridyl)-1,3,4-oxadiazole-2-thiol was dissolved in 25 mL of dilute hydrochloric acid by magnetic stirring. The above two were mixed and kept under stirring, employing a magnetic stirrer bar for 30 minutes. At low temperature of 60 °C, the homogeneous solution was allowed to evaporate slowly for 15–20 minutes and kept aside for 2 days when yellow crystals were formed. The excess solvent was decanted by filtration, and the crystals were washed with acetone.

Preparation of assembled gold nanostructures

The solid inclusion complex was prepared by adding equimolar solutions of Compound 1 and β-CD, sonicating the mixture in water at 120 rpm, warming at 60 °C for 30 minutes under atmospheric pressure in air, and then cooling at 4 °C for 2 days. The precipitate was filtered at the pump, washed and dried. 0.4 mM of Compound 1–β-CD inclusion complex was dissolved in 25 mL of methanol by magnetic stirring and 0.04 mM $HAuCl_4$ solution was added. Then, 0.2 mM $NaBH_4$ (ice-cold) solution was added drop wise to the mixture and stirred for 18 hours. The solvent was removed by freeze-drying. Finally, a lemon yellow coloured colloid of β-CD–capped thiol–gold nanocrystals was obtained.

Preparation of solutions

Owing to the poor solubility of Compound 1 in water, the stock solution was prepared in dilutehydrochloric acid. The final concentration of the Compound 1 used for taking spectral measurements was in the order of 10^{-6} M.

Preparation of colloidal gold solution

The β-cyclodextrin-thiol-gold nanocrystals were dispersed in ethanol and a stock solution was made. Test solutions were prepared by diluting the stock solution in water. The final solution contained 1% ethanol.

Instruments

UV–visible and fluorescence spectra were recorded using a Shimadzu 1800 spectrophotometer (Japan) and a JASCO FP–750 spectrofluorimeter (Japan) equipped with a 150W Xenon lamp for excitation respectively. Both the excitation and the emission band width were set up at 5 nm. Ultra-sonicator PCI 9L 250H, India was used for sonication. The surface topology was imaged by JEOL Model JSM 6360 scanning electron microscope (USA). The diffraction pattern of the inclusion complex was recorded using a Shimadzu XRD 6000 (Japan) using a monochromatic X-ray beam from Cu Kα radiation. Atomic force microscopic images were recorded on a Nanosurf Easyscan 2.0 instrument (Switzerland) on non-contact mode. Docking was performed using Schrodinger software to optimize the interaction of Compound **1** with β-CD. MOPAC-AM1 was utilized for viewing the thiol molecule for its feasibility of complexation with β-CD. The calculation of bond length between two atoms of thiol for the support of the results is executed in Fig. 1 (c).

RESULTS AND DISCUSSION
Inclusion complex formation of Compound 1 with β-cyclodextrin

The absorption spectra of Compound 1 (2.23 × 10^{-4} mol dm^{-3}) with various concentrations of β-CD from 0 mol dm^{-3} to 1.2 × 10^{-2} mol dm^{-3} at
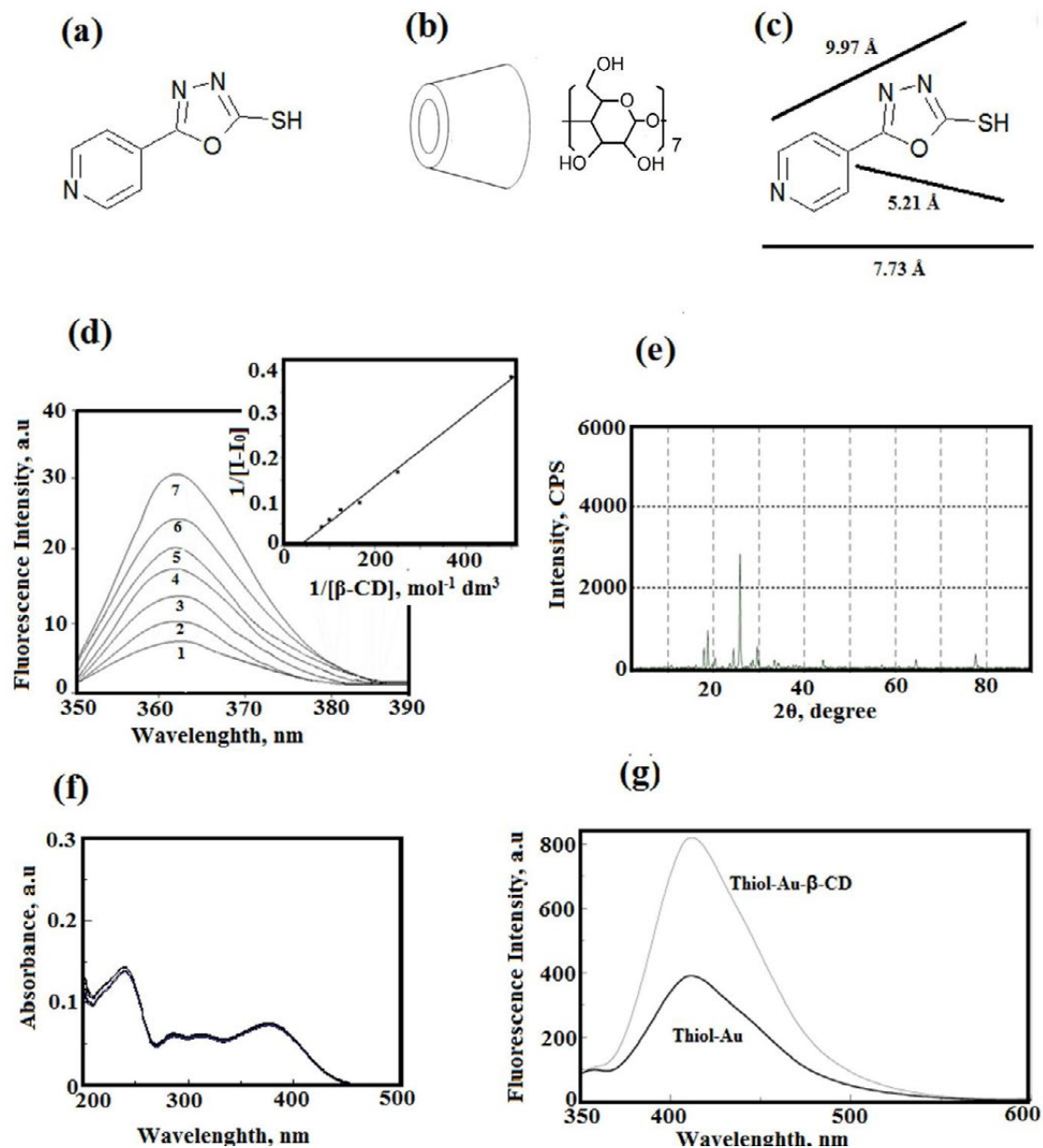
Fig. 1 (a) Molecular structure of 5-(4-pyridyl)-1,3,4-oxadiazole-2-thiol. (b) Structure of β-CD. (c) MOPAC-AM1 optimization of the dimensions of 5-(4-pyridyl)-1,3,4-oxadiazole-2-thiol. (d) Fluorescence enhancement on encapsulation of 5-(4-pyridyl)-1,3,4-oxadiazole-2-thiol by β-CD. The intensity increases at each addition of β-CD (in step-wise increasing concentration). Inset: The plot of $1/[$ β-CD] vs. $1/[I-I_0]$. (e) XRD pattern of 5-(4-pyridyl)-1,3,4-oxadiazole-2-thiol-β-CD inclusion complex. (f) UV-visible spectra of 5-(4-pyridyl)-1,3,4-oxadiazole-2-thiol with various added amounts of glucose. (g) Fluorescence enhancement on complex formation of 5-(4-pyridyl)-1,3,4-oxadiazole-2-thiol-Au nanostructures with β-CD.

different temperatures viz., room temperature of 25 °C, 30 °C, 35 °C, 40 °C ± 1 °C was analysed and given in Fig. 2. The absorbance of Compound 1 increases with respect to the addition of β-CD for all the temperature studied (Table 1). At room temperature, RT of 25 ± 1 °C, Compound 1 without the addition of β-CD show two prominent bands

viz., 239 and 375 nm (Fig. 2a). Table 1 show that the absorbance of Compound 1 enhances with stepwise increasing concentration of β-CD. The bands show blue shifts, due to the repositioning of Compound 1 from the polar water solvent environment to the hydrophobic cavity of β-CD [17]. There is a distinct isosbestic point at 368 nm

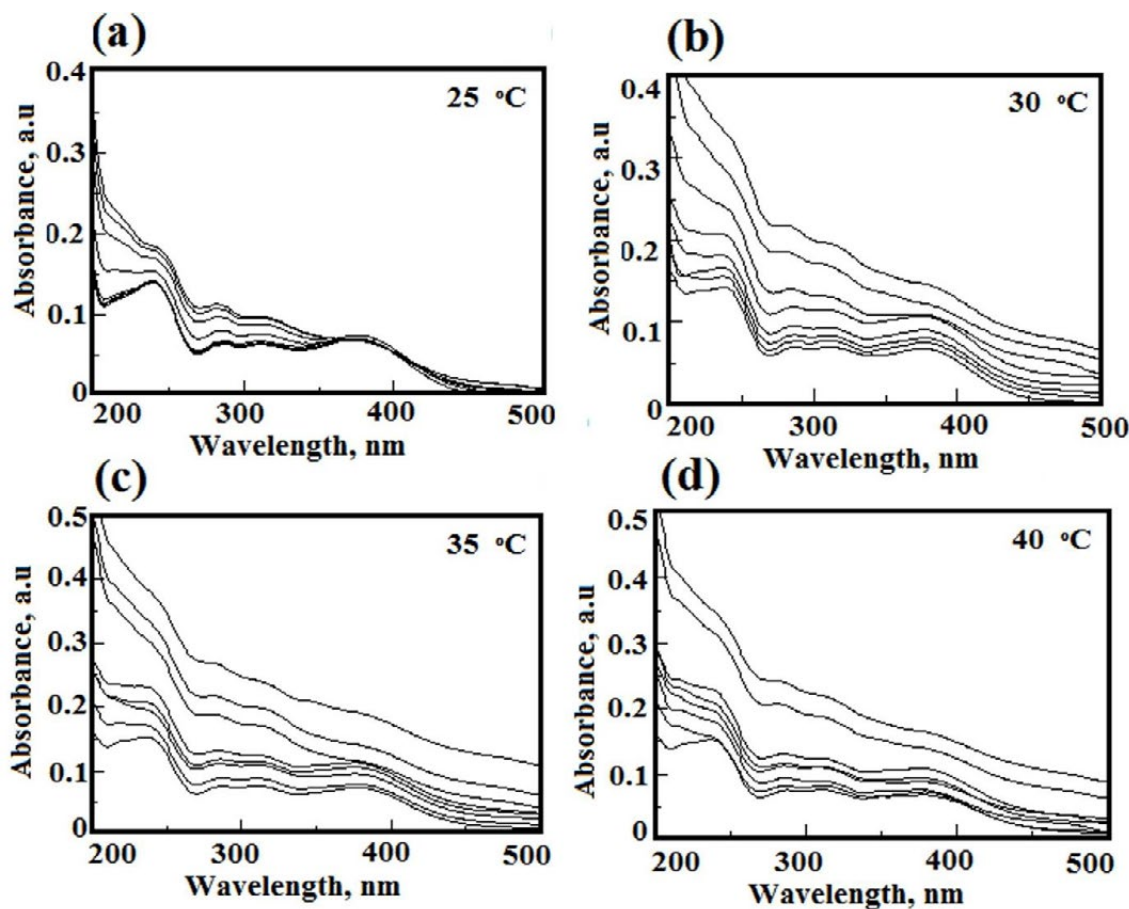Fig. 2. UV-visible spectra of 5-(4-pyridyl)-1,3,4-oxadiazole-2-thiol with various added amounts of β-CD at (a) 25 °C, (b) 30 °C, (c) 35 °C, and (d) 40 °C.

due to a binding equilibrium between Compound 1 and β-CD, given in equation 1 as follows.

$$\text{Compound 1} + \beta\text{-CD} \rightleftharpoons \text{Compound 1-}\beta\text{-CD} \qquad (1)$$

Fig. 1 (d) presents the fluorescence spectra of Compound 1 with various added amounts of β-CD (Table. 1). An aqueous solution of Compound 1 shows a fluorescence band at 364 nm at the excitation wavelength of 320 nm. Addition of β-CD enhances the fluorescence of the Compound 1 with a blue–shift of 2 nm. The enhancement of fluorescence is due to the host–guest complex formation. The stoichiometry and the binding constant of the host–guest complex are determined by performing a Benesi-Hildebrand plot (Fig. 1 (d) inset) [18]. The stoichiometry and the binding constant, K calculated are 1:1 and 1226 $mol^{-1} dm^3$ respectively. Complex formation involves the release of the water molecules from the CD cavity, voidance of the guest molecule of the polar hydration shell, entry of the guest into the empty CD cavity, and attainment of stability by weak van der Waals interactions. Hence, alterations of the enthalpic and entropic contributions occur in complex formation [18]. The restriction imposed on the guest molecule by the cavity of β-CD leads to an enhancement of fluorescence [19-20]. The IR spectra of Compound 1 and its β-CD inclusion complex are given in Fig. 3 (a) and 3 (b) respectively. The formation of Compound 1-β-CD inclusion complex results in the diminishing the transmittance of the corresponding bonds due to the non-covalent interactions such as hydrophobic interactions, Van der Waals forces, and hydrogen bonds. This is a general inference in the study of inclusion complexes by IR spectroscopy. The absence of new peaks in the Compound 1-β-CD inclusion complexes, in comparison to the Compound 1, rules out the possibility of formation of chemical bonds in the formed inclusion

complexes [21]. Compound 1 shows stretching vibrations of aromatic C–H (3032 cm⁻¹), aromatic C=C (1554 cm⁻¹), C–O (1365, 1330, 1234, 1215 and 1145 cm⁻¹), C–N (1053 and 1006 cm⁻¹), N–H (1597 cm⁻¹), S–H (2537 cm⁻¹), and deformation vibrations of C–H outside plane, aromatic rings (700–400 cm⁻¹) and C–O–C (1307 cm⁻¹). An appreciable change in the characteristic IR bands of Compound 1 is found at the formation of β-CD inclusion complex.

The inclusion of Compound 1 inside the cavity of β-CD is confirmed by theoretical approach of molecular modelling technique. The molecular modelling of Compound 1 with β-CD with a glide score of −2.29 K cal mol⁻¹ shown in Fig. 4 (a) to 4 (c) confirms their interactions by electrostatic, hydrogen bonding and hydrophobic mode of interactions respectively. The inclusion complexation of Compound 1 because of β-CD cavity is proven by treating Compound 1 in varying concentrations of glucose. Since no cavity is present in glucose, no changes are present in

interactions of Compound 1 with glucose observed (Fig. 1 (f)). The XRD data of β-CD were retrieved from the report by Farcas et.al [22]. The peaks of the Compound 1-β-CD formed are broadened and marginally different intensities are observed (Fig. 1 (e)). Using Debye–Scherrer formula (as given in equation 2) [23], the crystallite size is calculated.

$$D = \frac{0.9\lambda}{\beta\cos\theta} \qquad (2)$$

where D is the size of the crystal, λ is the wavelength of the radiation (=1.5418 Å), θ is the diffraction angle, and β represents the broadening factor (FWHM, Full width at half maximum). If the crystallite is strained then the *d* spacings will be changed. The approximate relationship relating the mean inhomogeneous strain (ε) to the peak broadening produces βε. It is derived by differentiating Bragg's law and relating the inhomogeneous strain to the differential δ*d/d*.

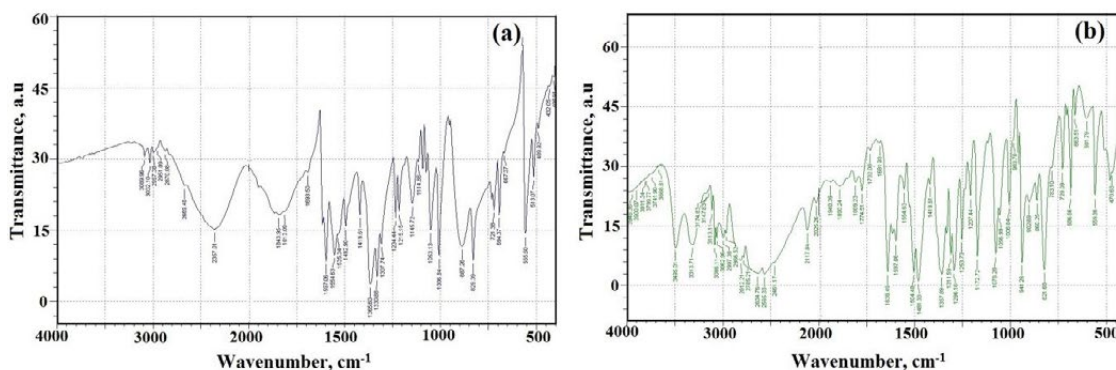
Fig. 3. IR spectra of (a) 5-(4-pyridyl)-1,3,4-oxadiazole-2-thiol and (b) 5-(4-pyridyl)-1,3,4-oxadiazole-2-thiol-β-CD complex.
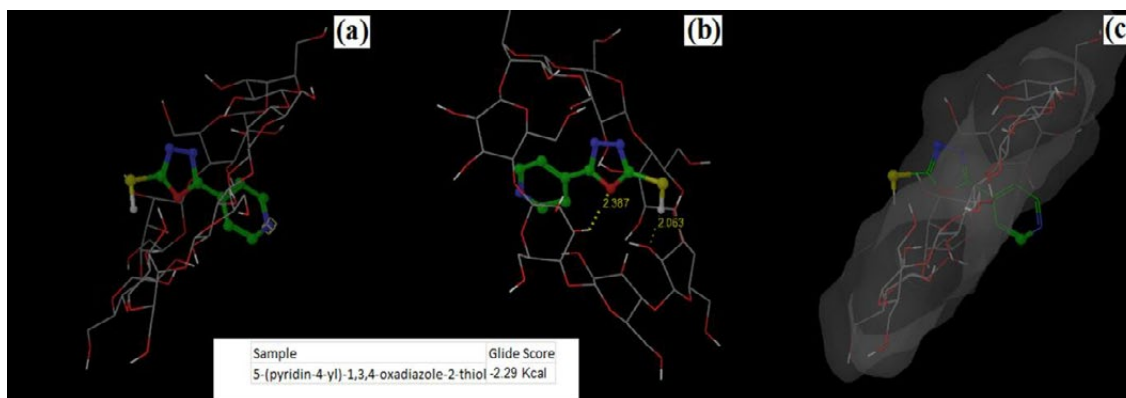

Fig. 4. Docking poses of (a) electrostatic, (b) hydrogen bonding, and (c) hydrophobic interactions in the β-CD complex of 5-(4-pyridyl)-1,3,4-oxadiazole-2-thiol.

The lattice strains from displacements of the unit cells about their standard positions. These are frequently produced by domain boundaries, dislocations, surfaces, etc. The peak broadening due to micro-strain will vary as given in equation (3) [24]:

$$B(2\theta) = \frac{4\varepsilon\sin\theta}{\cos\theta} \tag{3}$$

where B and ε represents the peak width and strain respectively. The crystallite size and strain for the Compound **1**-β-CD inclusion complex are 32 nm and 0.0047 respectively. But the crystallite size and strain for β-CD before encapsulating Compound **1** are 18 nm and 0.0011 respectively. This shows the formation of Compound **1**-β-CD inclusion complex by their interactions. In addition, the crystallite size of Compound **1**-β-CD inclusion complex is found very close to that of the physical size of the β-CD, which suggests that polycrystalline nanoparticles are not formed.

β-CD capping on thiol–assembled Au NPs nanostructures

Fig. 5 shows the absorption spectra of Compound **1** in the absence and the presence of gold structures. Acquiring of Au by Compound **1** is confirmed by 8 nm blue shift due to their interactions. The addition of various concentrations of β-CD to Compound **1**-Au resulted into increase in absorbance for all the temperature studied of 25 °C, 30 °C, 35 °C, 40 °C ± 1 °C (Fig. 6). A detailed fluorescence study on Compound **1**-Au at room temperature of 25 ± 1 °C with increase in concentrations of β-CD from 0 mol dm^{-3} to 1.2 × 10^{-3} mol dm^{-3} is given in Fig. 7 (a). The longer wavelength band (LW) does not get enhanced similar to the shorter wavelength band (SW) till the addition of 0.01 mol dm^{-3}. The band is characteristic of excimer or exciplex formation [25-26]. The formation of solvent exciplex, if any, can be identified from the fluorescence spectra of solvents of various polarities. Fig. 7 (b) shows the fluorescence spectra of Compound **1** recorded in various solvents. The dual fluorescence is observed in almost all the solvents, the LW band being notably prominent. A solvent exciplex cannot be expected in all the solvents. Thus, the LW band is attributed to the excimer of Compound **1** formed in solution. Quite rationally, the encapsulation of Compound **1** by β-CD prevents formation of self-aggregates of the guest molecule in solution. Thus, the β-CD complexation plays a role in the disruption of associative force between the thiol molecules. Contrary to such an association between the molecules of Compound **1**, β-CD molecules can self-assemble which, however, cannot be studied by optical methods. This assembly can happen in host–guest complex forms.
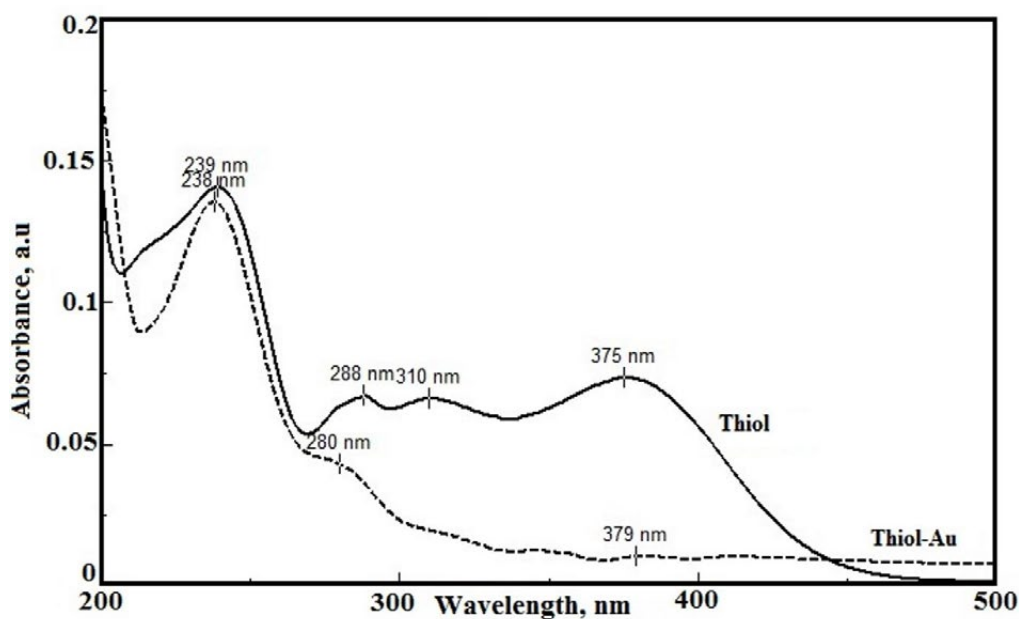

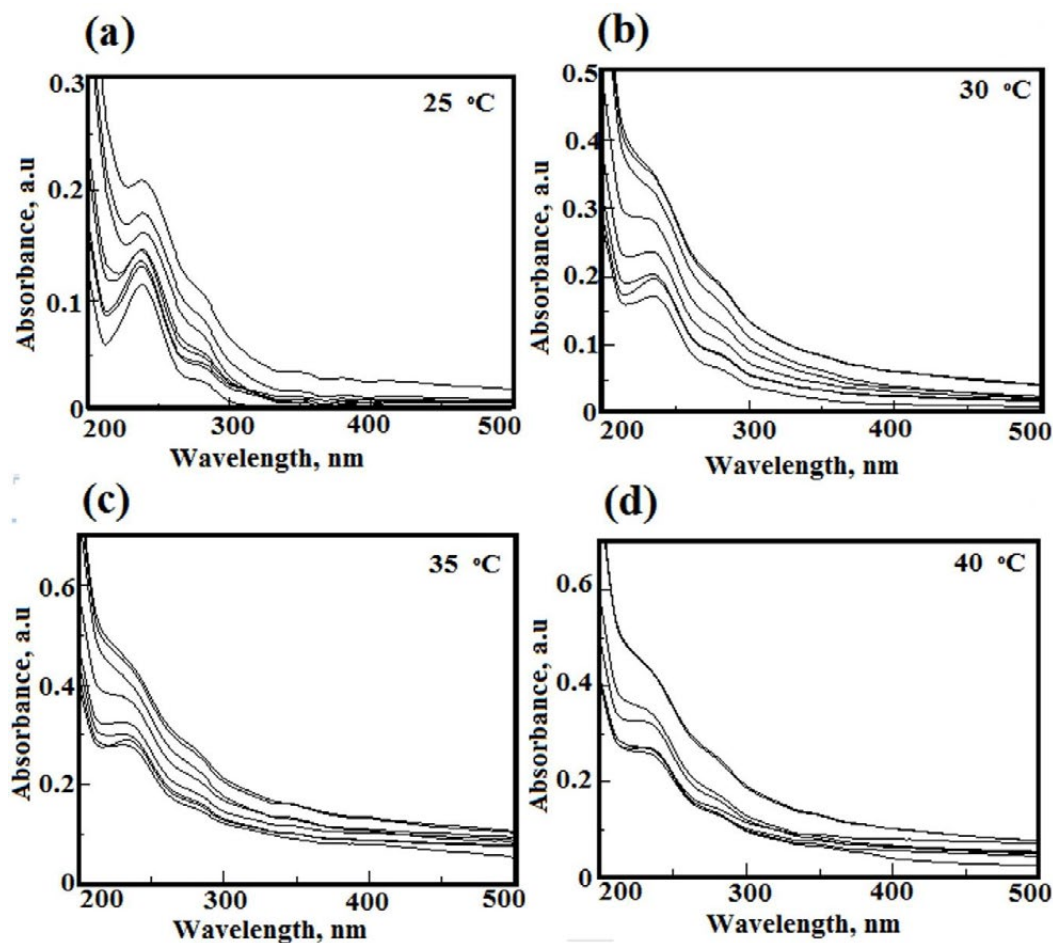Fig. 5. UV-visible spectra of 5-(4-pyridyl)-1,3,4-oxadiazole-2-thiol in free- and Au-linked forms.

Fig. 6. UV-visible spectra of 5-(4-pyridyl)-1,3,4-oxadiazole-2-thiol-Au with various added amounts of β-CD at (a) 25 °C, (b) 30 °C, (c) 35 °C, (d) 40 °C.

Morphology tuning of the nanostructure of thiol–assembled Au NPs

Customarily, the behaviour of nano-scale compounds is greatly sensitive to their dimension and shape [2-7]. We prepared the Au NPs reducing $HAuCl_4$ by $NaBH_4$ separately in the presence of Compound 1 and the Compound 1–β-CD complex (Fig. 1 (g)). An enhancement in the fluorescence intensity with a 3 nm red shift is observed on capping of β-CD onto thiol–assembled Au NPs nanostructures. The SEM images of the NPs are displayed in Fig. 8. The Compound 1 and Compound 1–Au NPs show irregular patterns due to the aggregated structures which fall in the range of around 1 µm (Fig. 8 (a) and 8 (b)). The aggregation is more clearly visible as 'ginger–like' structure in the AFM image of Compound 1–Au NPs (Fig. 9 (b)). When β-CD encapsulated

Compound 1 are imaged, rod–like patterned structures are seen (Fig. 8 (c)). Uniform organized host–guest structures provide driving forces for the formation of such commensurate structures. The mean size of the nanostructures is 72 ± 4 nm. An AFM image of the inclusion complex was recorded directly after the preparation of the complex. The structures of the complex look like associated units of doughnut shapes, seemingly being mid-way in the course of self-assembly to produce larger aggregates as seen in Fig. 9 (c). When the Compound **1**–β-CD complex is allowed to self–assemble on Au NPs in–situ during the preparation of Au NPs periodic spherical structures of Compound **1**–β-CD–Au NPs are formed. The size of the spheres is 370 ± 6 nm asin the SEM image in Fig. 8 (d). The AFM image shows a clearer picture of the spheres of Compound **1**–β-CD–Au
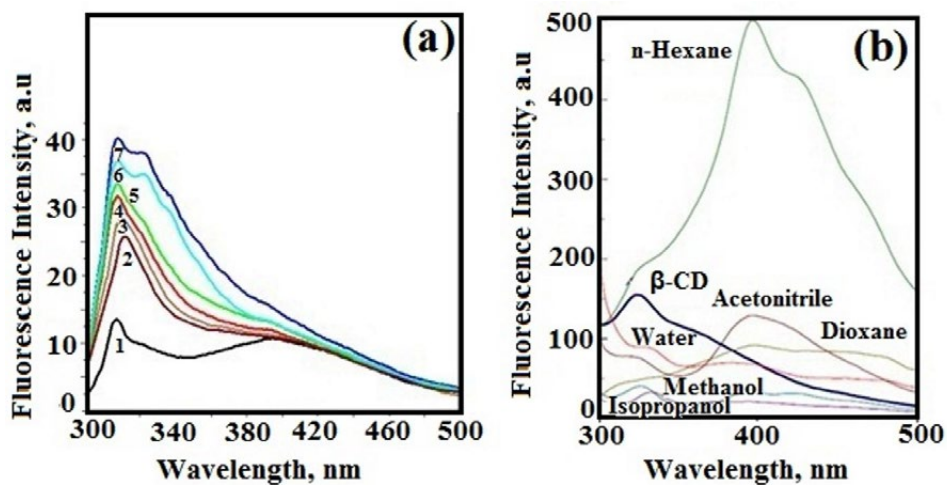
Fig. 7. (a) Fluorescence enhancement on inclusion complex formation of 5-(4-pyridyl)-1,3,4-oxadiazole-2-thi-ol-Au nanostructures with β-CD. Intensity increases at each addition of β-CD (in step-wise increasing concentration), (b) Fluorescence spectra of 5-(4-pyridyl)-1,3,4-oxadiazole-2-thiol in various solvents.
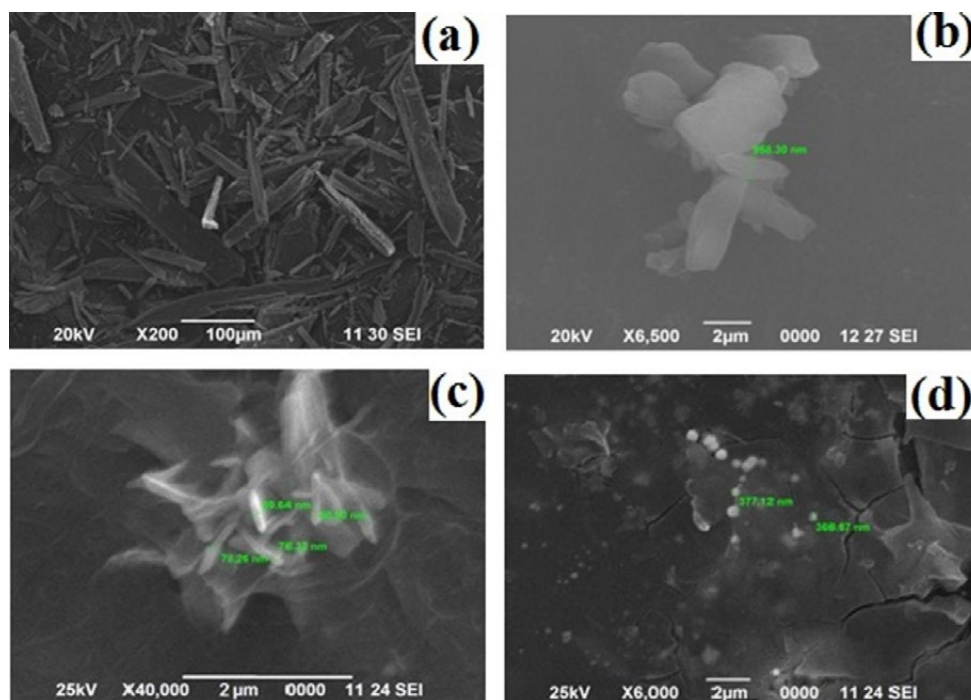

Fig. 8. SEM images of (a) 5-(4-pyridyl)-1,3,4-oxadiazole-2-thiol, (b) 5-(4-pyridyl)-1,3,4-oxadiazole-2-thiol-Au, (c) 5-(4-pyridyl)-1,3,4-oxadiazole-2-thiol-β-CD, (d) 5-(4-pyridyl)-1,3,4-oxadiazole-2-thiol-β-CD-Au.

NPs (Fig. 9(d)). The availability of the guest–β-CD complexes drives the formation of aggregates. The β-CD-to-β-CD association through hydrogen bonding allows the self-assembly governed by the chemical potential of the Compound **1**–β-CD–Au NPs in forming the spherical organized patterns. Therefore, the encapsulation of Compound **1** by β-CD modulates the mono-layered thiol–Au NP construct to adopt a commensurate structure. The surface characteristics and the formation
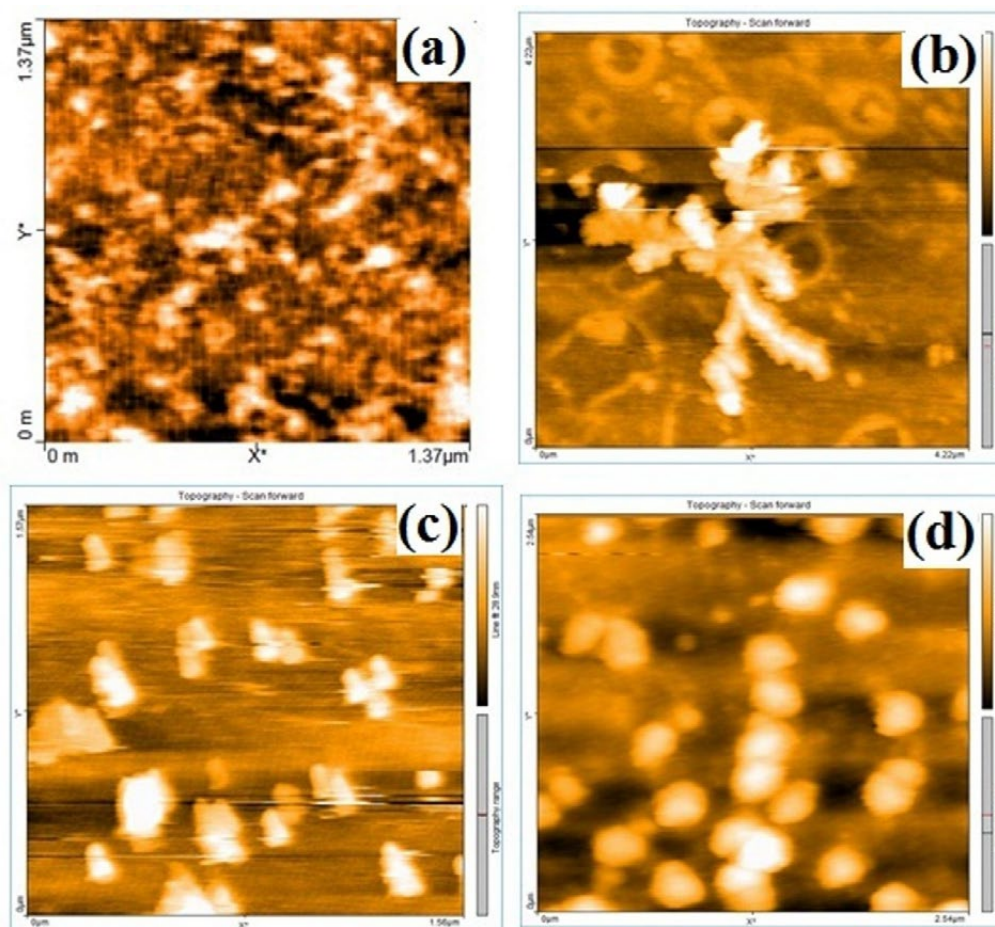
Fig. 9. AFM images of (a) 5-(4-pyridyl)-1,3,4-oxadiazole-2-thiol, (b) 5-(4-pyridyl)-1,3,4-oxadiazole-2-thiol-Au, (c) 5-(4-pyridyl)-1,3,4-oxadiazole-2-thiol-β-CD, (d) 5-(4-pyridyl)-1,3,4-oxadiazole-2-thiol-β-CD-Au.

of aggregates of molecule-on-nanoparticle self-assembled structures enact a crucial role in the targeted delivery of drugs.

CONCLUSIONS

β-Cyclodextrin forms a 1 : 1 inclusion complex with a thiol in aqueous medium with a binding constant of 1226 mol^{-1} dm^3. The thiol molecule and the thiol-β-CD assemble on the surface of Au NPs. The size of the thiol-Au NPs is 72 ± 4 nm and that of thiol-β-CD-Au NPs produce a larger structure (370 ± 6 nm). The morphology of the thiol-Au NPs is non-regular and that of thiol-**β-CD**-Au NPs is spherical. The self-assembly is supported by encapsulation of the thiol by β-CD. This occurs by the aggregation induced by the β-CD due to self-assembly. The nanoaggregate of the 5-(4-pyridyl)-1,3,4-oxadiazole-2-thiol therefore depends on whether it is assembled in bare form or β-CD-encapsulated form on the Au NPs.

CONFLICT OF INTEREST

The authors declare that there is no conflict of interests regarding the publication of this manuscript.

REFERENCES

1. Chen G, Roy I, Yang C, Prasad PN. Nanochemistry and Nanomedicine for Nanoparticle-based Diagnostics and Therapy. Chemical Reviews. 2016;116(5):2826-85.
2. Olajire AA, Adesina OO, Green Approach to synthesis of Pt and bimetallic Au@Pt nanoparticles using carica papaya leaf extract and their characterization. J. Nanostruct. 2017;7:338–344.
3. Thangaraj SE, Antony EJ, Yousuf S, Selvakumar PM, Dhanaraj P, Enoch IVMV. Binding interaction of a fluoranthene–thiol on gold nanoparticles with β-cyclodextrin and DNA. Journal of Experimental Nanoscience. 2016;12(1):62-71.
4. Kaykhaii M, Haghpazir N, Walisadeh J, Biosynthesis of gold

nanoparticles using aqueous extract of stem of Periploca aphylla plant. J. Nanostruct. 2018;8:152–158.

5. Jong WHD, Borm PJA. Drug delivery and nanoparticles: Applications and hazards. Int. J. Nanomed. 2008;3:133–149.

6. Xie H, Li H, Lai H, Wu W, Zeng X. Synthesis and antioxidative properties of a star-shaped macromolecular antioxidant based on β-cyclodextrin. Mater. Lett.2015;151:72–74.

7. Natesan S, Sowrirajan C, Dhanaraj P, Enoch IVMV. Capping of Silybin with β-Cyclodextrin Influences its Binding with Bovine Serum Albumin: A Study by Fluorescence Spectroscopy and Molecular Modeling. Bulletin of the Korean Chemical Society. 2014;35(7):2114-22.

8. Carneiro S, Costa Duarte F, Heimfarth L, Siqueira Quintans J, Quintans-Júnior L, Veiga Júnior V, et al. Cyclodextrin–Drug Inclusion Complexes: In Vivo and In Vitro Approaches. International Journal of Molecular Sciences. 2019;20(3):642.

9. Messner M, Kurkov SV, Flavià-Piera R, Brewster ME, Loftsson T. Self-assembly of cyclodextrins: The effect of the guest molecule. International Journal of Pharmaceutics. 2011;408(1-2):235-47.

10. Ferreira EB, Gomes JF, Tremiliosi-Filho G, Gasparotto LHS. One-pot eco-friendly synthesis of gold nanoparticles by glycerol in alkaline medium: Role of synthesis parameters on the nanoparticles characteristics. Materials Research Bulletin. 2014;55:131-6.

11. Iqbal M, Usanase G, Oulmi K, Aberkane F, Bendaikha T, Fessi H, et al. Preparation of gold nanoparticles and determination of their particles size via different methods. Materials Research Bulletin. 2016;79:97-104.

12. Liu M, Tang F, Yang Z, Xu J, Yang X. Recent Progress on Gold-Nanocluster-Based Fluorescent Probe for Environmental Analysis and Biological Sensing. Journal of Analytical Methods in Chemistry. 2019;2019:1-10.

13. Carnegie C, Chikkaraddy R, Benz F, de Nijs B, Deacon WM, Horton M, et al. Mapping SERS in CB:Au Plasmonic Nanoaggregates. ACS Photonics. 2017;4(11):2681-6.

14. Sierpe R, Lang E, Jara P, Guerrero AR, Chornik B, Kogan MJ, et al. Gold Nanoparticles Interacting with β-Cyclodextrin–Phenylethylamine Inclusion Complex: A Ternary System for Photothermal Drug Release. ACS Applied Materials & Interfaces. 2015;7(28):15177-88.

15. Xu S, Hartvickson S, Zhao JX. Engineering of SiO2–Au–SiO2Sandwich Nanoaggregates Using a Building Block: Single, Double, and Triple Cores for Enhancement of Near

Infrared Fluorescence. Langmuir. 2008;24(14):7492-9.

16. Kim JH, Kim KS, Manesh KM, Santhosh P, Gopalan AI, Lee K-P. Self-assembly directed synthesis of gold nanostructures. Colloids and Surfaces A: Physicochemical and Engineering Aspects. 2008;313-314:612-6.

17. Yousuf S, Alex R, Selvakumar PM, Enoch IVMV, Subramanian PS, Sun Y. Picking Out Logic Operations in a Naphthalene β-Diketone Derivative by Using Molecular Encapsulation, Controlled Protonation, and DNA Binding. ChemistryOpen. 2015;4(4):497-508.

18. Koshland DE. The Key–Lock Theory and the Induced Fit Theory. Angewandte Chemie International Edition in English. 1995;33(2324):2375-8.

19. Yousuf S, Enoch I. Spectroscopic investigation of interaction of 6-methoxyflavanone and its β-cyclodextrin inclusion complex with calf thymus DNA. Chemical Papers. 2012;66(8).

20. Sudha N, Sameena Y, Chandrasekaran S, Enoch IVMV, Premnath D. Alteration of the Binding Strength of Dronedarone with Bovine Serum Albumin by β-Cyclodextrin: A Spectroscopic Study. Spectroscopy Letters. 2014;48(2):112-9.

21. Pereira R, Andrades N, Paulino N, Sawaya A, Eberlin M, Marcucci M, et al. Synthesis and Characterization of a Metal Complex Containing Naringin and Cu, and its Antioxidant, Antimicrobial, Antiinflammatory and Tumor Cell Cytotoxicity. Molecules. 2007;12(7):1352-66.

22. Farcas A, Jarroux N, Farcas AM, Harabagiu V, Guegan P. Synthesis and Characterization of Furosemide Complex in β-Cyclodextrin. Digest J. Nanomat. Biostruct. 2006;1, 55–60.

23. Langford JI, Wilson AJC. Scherrer after sixty years: A survey and some new results in the determination of crystallite size. Journal of Applied Crystallography. 1978;11(2):102-13.

24. He K, Chen N, Wang C, Wei L, Chen J. Method for Determining Crystal Grain Size by X-Ray Diffraction. Crystal Research and Technology. 2018;53(2):1700157.

25. Thiagarajan V, Selvaraju C, Malar EJP, Ramamurthy P. A Novel Fluorophore with Dual Fluorescence: Local Excited State and Photoinduced Electron-Transfer-Promoted Charge-Transfer State. ChemPhysChem. 2004;5(8):1200-9.

26. Enoch MV, Rajamohan R, Swaminathan M. Fluorimetric and prototropic studies on the inclusion complexation of 3,3'-diaminodiphenylsulphone with β-cyclodextrin and its unusual behavior. Spectrochimica Acta Part A: Molecular and Biomolecular Spectroscopy. 2010;77(2):473-7.